Journal of Alzheimer's Disease 22 (2010) 909–922
DOI 10.3233/JAD-2010-100678
IOS Press

Increased Cortical Thickness and Caudate Volume Precede Atrophy in *PSEN1* Mutation Carriers

Juan Fortea[a], Roser Sala-Llonch[b,c], David Bartrés-Faz[b,c], Beatriz Bosch[a], Albert Lladó[a,c], Nuria Bargalló[c,d], José Luis Molinuevo[a,c] and Raquel Sánchez-Valle[a,c,*]
[a]*Alzheimer's Disease and Other Cognitive Disorders Unit, Neurology Service, Hospital Clínic, Barcelona, Spain*
[b]*Department de Psiquiatria i Psicobiologia Clinica, Universitat de Barcelona, Spain*
[c]*Institut d'Investigació Biomédica August Pi i Sunyer (IDIBAPS), Barcelona, Spain*
[d]*Radiology Service, Hospital Clínic de Barcelona, Spain*

Accepted 27 July 2010

Abstract. Neuroimaging studies of familial Alzheimer's disease allow investigation of the disease process before clinical onset. We performed semi-automated MRI analysis to evaluate cortical thickness (CTh), grey matter (GM) volumes, and GM diffusivity indexes in *PSEN1* mutation carriers (MC). We recruited 11 MC from 4 families with *PSEN1* mutations (L286P, M139T, K239N) and 6 familial and 12 non-familial healthy controls. MC were classified as either asymptomatic ($n = 6$) or symptomatic ($n = 5$). Subjects underwent structural and diffusion-weighted 3-Tesla MRI scanning. CTh and GM volumes of subcortical structures and diffusivity indexes were calculated and group comparisons were performed. Structural images were reanalyzed with voxel-based morphometry methodology. Cerebrospinal fluid amyloid-β_{1-42} levels (Aβ) were measured. We found that symptomatic MC presented widespread cortical thinning, especially in precuneus and parietotemporal areas ($p < 0.01$) and increased mean diffusivity (MD) in these areas compared to controls. Unexpectedly, asymptomatic MC, 9.9 years prior to the predicted age of disease onset, presented increased CTh in the precuneus and parietotemporal areas ($p < 0.01$), increased caudate volumes ($p < 0.01$), and decreased MD ($p < 0.05$) in these areas compared to HC. In MC, CTh correlated with adjusted age. Aβ values were within normal limits in AMC. In conclusion, at early preclinical stages, CTh in the precuneus and parietotemporal regions and caudate volume increase in *PSEN1* MC and decrease thereafter with disease progression. The different trends in MD in asymptomatic and symptomatic MC suggest that different microstructural changes underlie the contrasting morphometric findings. Reactive neuronal hypertrophy or/and inflammation may account for increased CTh and decreased MD in asymptomatic MC.

Keywords: Alzheimer disease, amyloid, cerebrospinal fluid, magnetic resonance imaging, presenilin 1

INTRODUCTION

Most Alzheimer's disease (AD) cases are sporadic, typically occurring in persons over 65 years of age. However, a minority of AD cases are inherited with an autosomal dominant pattern. Genetic defects in three genes have so far been described in these inherited forms: the amyloid-β protein precursor (*AβPP*), the presenilin-1 (*PSEN1*), and the presenilin-2 (*PSEN2*) [1]. These forms have an early age of onset, which is relatively predictable, with nearly 100% penetrance. These forms constitute, therefore, an ideal scenario with few confounding factors to study the preclinical stage of the disease.

Functional neuroimaging has revealed functional al-

*Correspondence to: Raquel Sánchez-Valle, Alzheimer's Disease and Other Cognitive Disorders Unit, Neurology Service, Hospital Clínic, Villarroel 170, 08036 Barcelona, Spain. Tel.: +34 932275785; Fax: +34 932275783; E-mail: rsanchez@clinic.ub.es.

ISSN 1387-2877/10/$27.50

terations in the target brain AD areas as long as 30 years prior to the mean familial age of disease onset [2], and MR spectra have shown metabolite abnormalities a decade before the expected onset [3]. Structural changes such as medial temporal or global brain atrophy [4], or accelerated rate of grey matter (GM) loss [5], have also been found in mutation carriers (MC) years before clinical onset, although brain atrophy seems to occur later than functional abnormalities [6].

Recently, new methods have been developed for the measurement of cortical thickness (CTh) across the entire mantle that have proven their usefulness in detecting widespread abnormalities in early phases of sporadic AD [7], even in asymptomatic subjects in whom positive amyloid binding suggests cortical amyloid deposition [8]. This technique has proved useful in assessing subtle structural longitudinal changes in *AβPP* and *PSEN1* MC, finding a decrease in CTh in the posterior cingulate and in the precuneus prior to symptom onset [9].

Diffusion tensor imaging (DTI) is a technique that allows investigation of brain microstructure integrity based on the directionality of the diffusion of water molecules. Mean diffusivity (MD) provides a scalar measure of total diffusivity. Although it has been more widely studied in white matter, MD can also be used in the study of the integrity of grey matter in AD and mild cognitive impairment patients [10]. In this sense, in a recent study in healthy elderly, changes in MD predicted memory performance, whereas volume changes did not [11].

The aim of the present study was to analyze the CTh and subcortical GM structure volumes and GM diffusivity indexes in symptomatic and asymptomatic *PSEN1* MC.

MATERIALS AND METHODS

Participants

Eleven mutation carriers from 4 families with 3 different *PSEN1* mutations (M139T, L286P, K239N) were recruited from the genetic counseling program for familial dementias (PICOGEN) at the Hospital Clinic, Barcelona, Spain. These mutations have been published elsewhere [1,12,13]. All the subjects approached already knew their at-risk status for genetic AD. At-risk subjects received a session of genetic counseling and were given the option of knowing their genetic status through the genetic counseling protocol. Six at risk individuals who were found to be non carriers and twelve healthy volunteers, age- and gender-matched to the asymptomatic MC (AMC), were also recruited to increase the statistical power of the sample. The study was approved by the local ethics committee and all subjects gave informed written consent.

Clinical and neuropsychological characterization

Subjects underwent clinical and cognitive evaluations. The comprehensive neuropsychological battery included verbal and visual memory (Free and Cued Selective Reminding Test-FCSRT and Rey-Osterrieth Complex Figure), semantic memory (animals fluency), language (Boston Naming Test and language comprehension of the Boston diagnostic Aphasia Battery-), praxis (ideomotor praxis and constructive praxis from the Consortium to Establish a Registry for Alzheimer's Disease (CERAD), visual perception (incomplete letters and number location subtest from Visual Object and Space Perception Battery-VOSP) and frontal function (Controlled Oral Word Association Test- COWAT, Trail Making Test part A and B, digit span) assessment was used. The Pfeffer Functional Activities Questionnaire (FAQ) was used for assessing patients' functional activities. Subjects were classified clinically as asymptomatic if they had no memory complaints, a normal cognitive evaluation and the Clinical Dementia Rating (CDR) scale performed with an informant was 0; or symptomatic if cognitive performance was more than 1.5 SD below the mean respect their age and education level in any cognitive test or CDR > 0. Symptomatic MC (SMC) were further classified as non-demented (SMC-ND) if CDR $= 0.5$ or demented (SMC-D) if CDR $\geqslant 1$.

This study included four families with three different mutations, with different median ages of onset (46, 40, and 52.5 years respectively). Because PSEN1 MC have an early age of onset with nearly 100% penetrance and a relatively predictable age of onset within a given family we defined and calculated for each MC the adjusted age as the subject's age relative to the median familial age of onset.

Genetic analysis

Genomic DNA was extracted from peripheral blood of probands using the QIAamp DNA blood minikit (Qiagen). Mutation screening was performed as previously described [12].

Apolipoprotein E (*APOE*) genotyping was performed by polymerase chain reaction amplification and *Hha*I restriction enzyme digestion.

CSF analysis

CSF study was offered to at-risk individuals. CSF was obtained and processed according to standard protocols. CSF Aβ_{1-42} concentrations were determined by ELISA, provided by Innogenetics®, Gent, Belgium (Innotest β-amyloid 1-42).

MRI acquisition

Subjects were examined on a 3T MRI scanner (Magnetom Trio Tim, Siemens Medical Systems, Germany). A high resolution 3D structural dataset (T1-weighted MP-RAGE, TR = 2300 ms, TE = 2.98 ms, 240 slices, FOV = 256 mm; matrix size = 256 × 256; Slice thickness = 1 mm) was acquired for the 29 subjects included. The DWI protocol consisted of an echo-planar imaging (EPI) sequence (30 directions+b0 image, with 2 repeated acquisitions, TR = 7600 ms, TE = 89 ms, 60 slices, slice thickness = 2 mm, distance factor = 0%, FOV = 250 mm, matrix size = 122 × 122, voxel size = 2 × 2 × 2 mm).

Cortical thickness and volumetric segmentation procedures

Cortical reconstruction and volumetric segmentation of the structural images was performed with the FreeSurfer image analysis suite, version 4.3.1 (http://surfer.nmr.mgh.harvard.edu). The procedures have been fully described elsewhere [14]. In short, reconstructed and registered individual CTh maps were smoothed using a Gaussian kernel of 20 mm Full-Width Half Maximum and introduced in a group analysis, based on general linear modeling (GLM) of the data (age, gender, and family were introduced as covariates). Regions that presented significant differences between groups were used to define regions of interest (ROI) for analysis in further region-specific studies. We also manually drew another ROI in the primary visual cortex to serve as a control structure (VisualROI) [8]. Furthermore, within the FreeSurfer streamline, a parcellation of each individual surface was performed with two different atlases available [15,16]. Mean thickness of the parcellations of interest were used to do between-groups comparisons, and regression analysis with adjusted age.

Subcortical segmentation was performed also as implemented in FreeSurfer. The segmentation procedure allows the obtainment of a measure of the estimated Intracranial Volume (EIV) [17], which is based on the scale factor used for the atlas registration. Finally, GM volumes for all the subcortical segmented structures were extracted for each subject.

CTh analyses were done with and without a correction for multiple comparisons. The uncorrected results were thresholded at $p < 0.01$ level. We performed two different kinds of multiples comparison correction. First a FDR multiple comparison correction was applied. Moreover a Familywise Error (FWE) permutation testing (500 permutations) was performed, as implemented in FreeSurfer.

Voxel based morphometry (VBM) analysis

Structural MRI data were also processed with FSL-VBM stream protocol, a voxel-based morphometry style analysis included in the FSL suite (http://www.fmrib.ox.ac.uk/fsl) [18]. Procedures within this protocol allow an accurate voxelwise comparison of individual grey matter maps, using GLM (age, gender, and family were introduced as covariates) and permutation-based non-parametric testing and correcting for multiple comparisons across space, using family-wise error (FWE) correction.

Analysis of diffusion MRI data

Diffusion MRI was processed using tools implemented in FSL. First, individual MD maps were extracted for each subject. These maps were registered to MNI152 space and introduced into a GLM analysis to perform group comparisons. Appropriate registration tools were applied to extract mean MD values in the different ROIs. MD analyses using a cortical mask are presented corrected for multiple comparisons, using FWE algorithm, and thresholded at $p < 0.05$ level of significance.

Statistical analysis

Group analyses were made using the Statistical Package for Social Sciences (SPSS) v.16 (Chicago, Il, USA). Comparisons between groups (SMC/AMC versus HC) were performed using two-tailed t-tests

RESULTS

Demographic and clinical characteristics and genetic status

Demographic data and *APOE* genotype of all partic-

Table 1
Demographic data of the participants

	Subject	Family	Gender	Age (years)	Relative age (years)	CDR sum of boxes	MMSE	*APOE*
SMC group	SMC1	1	Female	38	−1.99	2	28	33
	SMC2	1	Female	45	5.36	5,5	24	33
	SMC3	1	Male	43	3.15	2,5	24	33
	SMC4	2	Male	51	4.98	10	17	43
	SMC5	3	Female	60	7.27	14	11	33
AMC group	AMC1	2	Male	33	−12.79	0	30	33
	AMC2	2	Female	32	−14	0	30	23
	AMC3	3	Female	45	−7.4	0	29	33
	AMC4	3	Female	49	−3.58	0	27	33
	AMC5	3	Female	55	2.97	0	29	33
	AMC6	4	Male	33	−12.3	0	28	33
HC group	HC1	1	Female	44	–	0	29	43
	HC2	1	Female	35	–	0	30	33
	HC3	1	Female	39	–	0	29	33
	HC4	3	Female	52	–	0	29	33
	HC5	4	Female	25	–	0	29	33
	HC6	4	Male	35	–	0	29	33
	Non-familiar HC group N = 12		Male 4/ Female 8	42.08 ± 11.59	–	0	29.44 ± 0.511	

ipants is summarized in Table 1. Five MC were SMC (2 SMC-ND and 3 SMC-D) with a median age of 45 years (range 38–60 years), median adjusted age of 5.0 years (range −1.9–7.3 years). Six MC were AMC with a median age of 39 years (range 32–55 years) and median adjusted age of −9.9 (range −14.0 to 3.0 years), and 18 participants were HC (median age 39.4 years; range 25.2 to 59.8 years). Age, education, gender, and MMSE did not differ between HC and AMC. As expected, SMC were older than HC and AMC and presented significant differences on all clinical and functional scales.

Four SMC and 3 AMC consented to participate in the study of CSF Aβ levels. The 4 SMC presented abnormally low values (mean 175 pg/mL), while AMC presented normal values (mean 776 pg/mL).

Structural analysis

The estimated intracranial volume (EIV) did not differ between HC and AMC (1475790 mm^3 versus 1488259 mm^3, $p = 0.87$) or between HC and SMC (1463620 mm^3, $p = 0.89$). EIV was therefore not included in subsequent statistical models.

Cortical thickness analysis in symptomatic and asymptomatic mutation carriers

Analysis of whole brain CTh maps revealed significant thinning ($p < 0.01$ uncorrected) in SMC in many areas across the entire cortical mantle (*SympROI*). A separate analysis between HC and both SMC-ND and SMC-D was performed (Fig. 1). The difference maps between HC and each subgroup showed that although the pattern of thinning in the SMC-ND was similar to that of SMC-D, its extension and magnitude was clearly lower than in SMC-D. The posterior cingulate and precuneus (PPC) and posterior association areas – the superior temporal gyrus (ST), the banks of the superior temporal sulcus (BSTS), inferior and superior parietal cortex (IP and SP), fusiform gyrus (FG) – presented more severe and widespread cortical thinning than frontal areas where the thinning appeared more restricted to certain specific regions (anterior cingulate, pars triangularis, pars orbitalis, frontal pole, orbitofrontal, and superior frontal). There were minor differences in the spatial location of regional thinning across hemispheres, but the results were quite consistent bilaterally. We also found a region of focal cortical thickening in the anterior right cingulate cortex present in both SMC-ND and SMC-D patients when compared to HC.

Figure 2 shows the difference maps for the AMC group in comparison with the HC group. Only small scattered areas of cortical thinning across the cortex appeared. Unexpectedly, several regions – the PPC, the BSTS, the IP, the SP and the FG – showed cortical thickening. Some of these regions (precuneus, BSTS, supramarginalis and IP areas) survived the FWE multiple comparison correction which are shown in Table 2 and a region in the PPC also survived FDR correction (shown in Fig. 3). Uncorrected differences are repre-

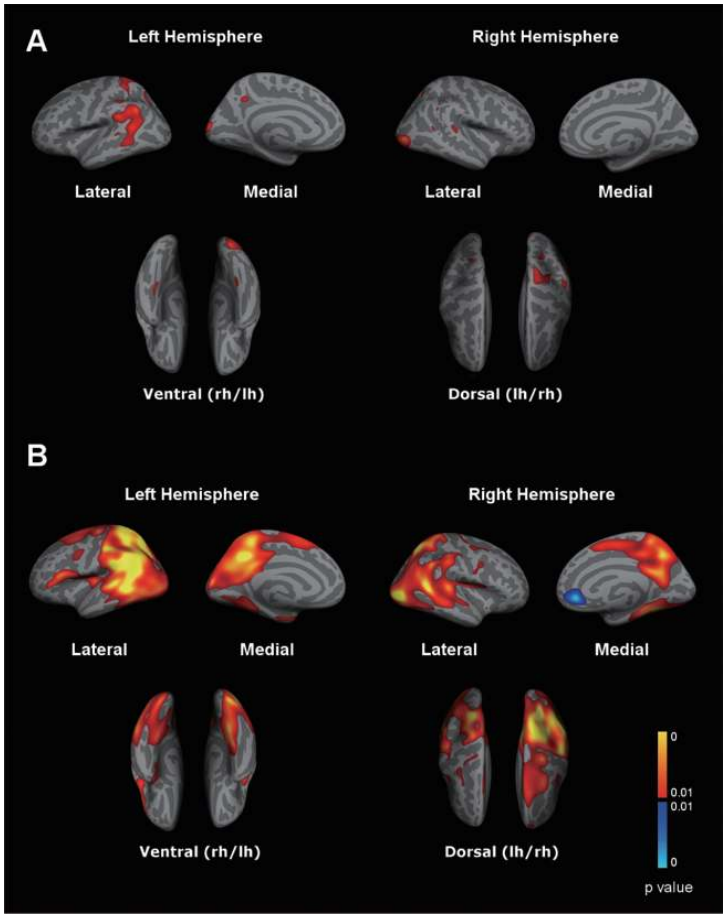

Fig. 1. Cortical thickness (CTh) difference maps in different clinical stages: (A) Non-demented symptomatic mutation carriers, (B) Demented symptomatic mutation carriers. Both compared against the healthy control group ($p < 0.01$ uncorrected). Red-yellow color code means decreased CTh, and blue color code means increased CTh.

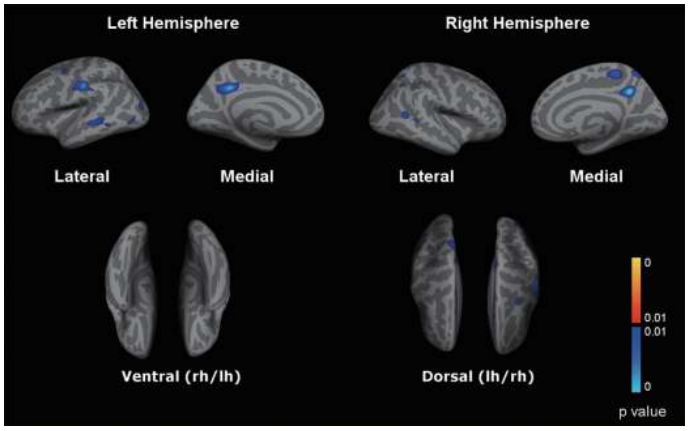

Fig. 2. Cortical thickness (CTh) difference maps for the contrast AMC versus HC. Thresholded at $p < 0.01$, uncorrected. Red-yellow color code means decreased CTh, and blue color code means increased CTh.

Table 2
Familywise Error (FWE) multiple comparisons correction (500 permutations). Cortical areas corresponding to each cluster were assigned using the parcellations from an available atlas [15] BTSS = banks of the temporal superior sulcus

Cluster number	Size (mm^2)	Max p value	Max-p Tailarach coordinates	Cluster-Wise probability	Cluster-Wise confidence interval	Atlas label
1	613.75	$10^{(-5.2)}$	(−14.3, −46.1, 30.5)	0.05	[0.038–0.062]	precuneus
2	766.89	$10^{(-3.6)}$	(−49.4, −41.8, 1.3)	0.01	[0.004–0.016]	BTSS
3	876.53	$10^{(-3.6)}$	(−53.1, −35.8, 29.7)	0.002	[0.000–0.004]	supramarginal
4	1102.14	$10^{(-3.2)}$	(−29.0, −80.5, 15.3)	0.002	[0.000–0.004]	inferiorparietal

Table 3
Average Cortical Thickness (CTh) and group comparisons within the defined regions of interest. AsympROI refers to areas with increased CTh in the AMC group, SympROI refers to areas with reduced CTh in the SMC group, and VisualROI serves as a control region

Average CTh (mm)		*SympROI* Mean (SD)	*AsympROI* Mean (SD)	*VisualROI* Mean (SD)
HC		2.55 (0.09)	2.38 (0.08)	1.62 (0.15)
AMC		2.66 (0.09)	2.64 (0.18)	1.57 (0.11)
SMC	Non-demented	2.31 (0.05)	2.26 (0.09)	1.46 (0.12)
	Demented	2.04 (0.07)	1.93 (0.06)	1.37 (0.08)
Group Comparisons				
HC vs AMC		$t = 2.5, p = 0.019$	$t = 5.06, p < 0.001$	$t = 0.69, p = 0.5$
HC vs SMC-ND		$t = 3.49, p = 0.003$	$t = 2.04, p = 0.057$	$t = 1.38, p = 0.18$
HC vs SMC-D		$t = 9.06, p < 0.001$	$t = 9.63, p < 0.001$	$t = 2.6, p = 0.015$

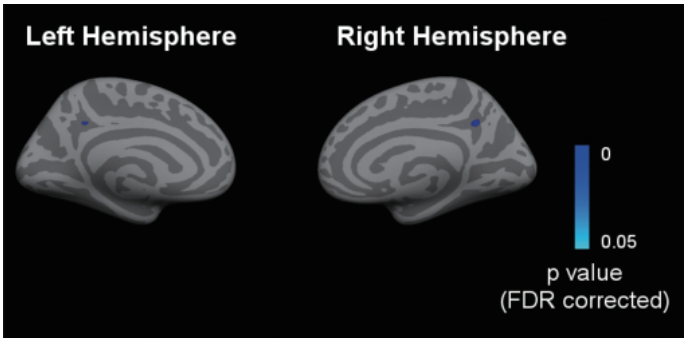

Fig. 3. Cortical thickness (CTh) difference maps for the contrast AMC versus HC. FDR multiple comparison correction thresholded at $p < 0.05$. Blue color code means increased CTh.

sented in Fig. 2 when compared to HC. *AsympROI* was created from the map at p<0.01.

Table 3 shows the mean CTh values for each group in the 3 ROIs (*SympROI, AsympROI* and *VisualROI*). SMC-D presented a 20% decrease in *SympROI* and 18.9% in *AsympROI* compared to HC ($p < 0.001$ and $p < 0.01$ respectively), more severe than SMC-ND cortical thinning (5.047% in *AsympROI* and 9.41% in *SympROI*). In AMC, mean CTh presented 10.9% and 4.31% increases in both *AsympROI* and *SympROI* areas when compared to HC ($p < 0.001$ and $p = 0.019$ respectively). These changes were not found in the control region *VisualROI*, where only SMC-D presented differences with HC. We found the same type of changes when determining CTh in several automatically atlas derived regions (Table 4).

We found an overlap between the *SympROI* and the *AsympROI*, although the extension of cortical thinning in SMC was greater than that of cortical thickening in AMC (Fig. 4).

Figure 5 presents individual mean CTh values in the *AsympROI*. Most MC values fall outside the range of HC values, with higher values for individual mean CTh in AMC and lower values in SMC. We used the individual CTh values extracted from the *AsympROI* to examine the relationship between the adjusted age and CTh. There was no correlation between absolute age and CTh in HC. However, a strong correlation

Table 4
Average Cortical Thickness (CTh) and group comparisons within the atlas-based regions of interest [16]. Regions are represented in Fig. 6

	CTR	AMC	t-test (CTR vs AMC)	SMC	T-test (CTR vs SMC)
right_S_subparietal	2.42(0.16)	2.63(0.14)	T = 2.85, $p = 0.009$	2.09(0.29)	$t = 3.17$, $p = 0.005$
left_S_subparietal	2.38(0.11)	2.54 (0.19)	T = 2.44, $p = 0.023$	1.83(0.28)	$t = 6.71$, $p = 0.000$
left_S_occipital_middle_and_Lunatus	2.10(0.16)	2.30(0.15)	T = 2.51, $p = 0.020$	1.66(0.20)	$t = 4.65$, $p = 0.000$
left_S_occipital_superior_and_transversalis	2.15(0.16)	2.32(0.09)	T = 2.57, $p = 0.018$	1.81(0.28)	$t = 3.37$, $p = 0.003$
left_S_Cingulate_marginalis	2.21(0.15)	2.36(0.14)	T = 2.1, $p = 0.047$	1.77(0.22)	$t = 4.97$, $p = 0.000$

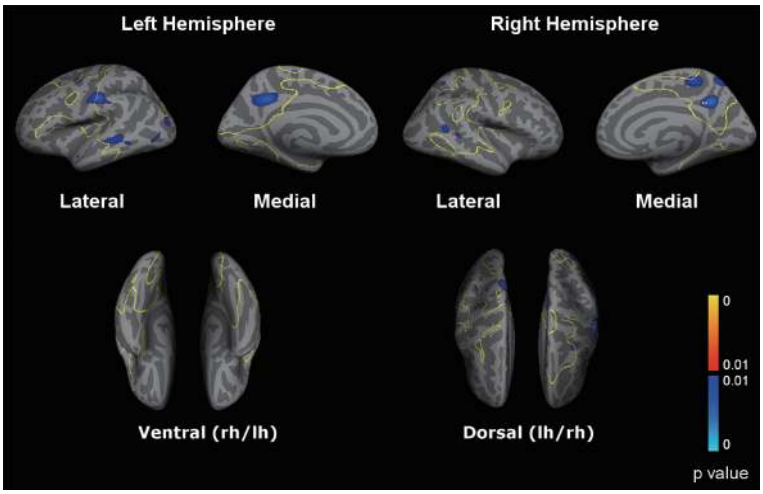

Fig. 4. Overlap of AMC versus HC (dark blue-light blue), and SMC versus HC (yellow lines) difference maps.

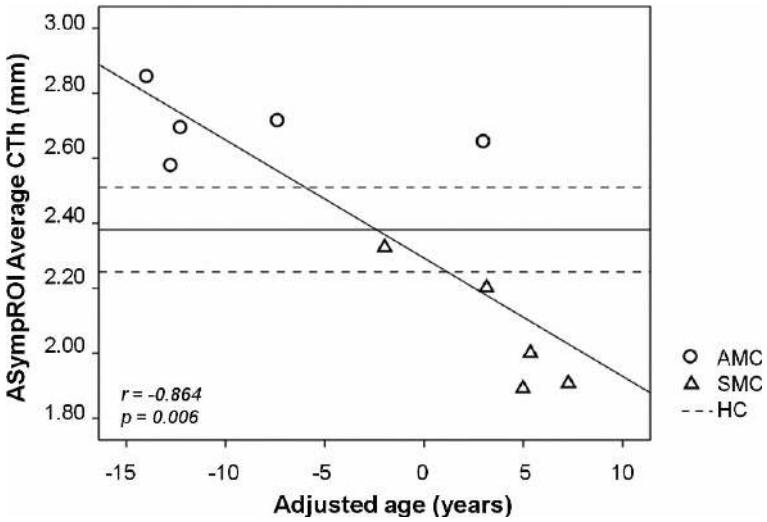

Fig. 5. Correlation between mean cortical thickness (CTh) values measured in the AsympROI and adjusted age of each mutation carrier (asymptomatic carriers in circles, symptomatic carriers in triangles). Solid line is the adjusted regression line. Solid and dashed lines represent mean CTh and its range measured in the same ROI for HC.

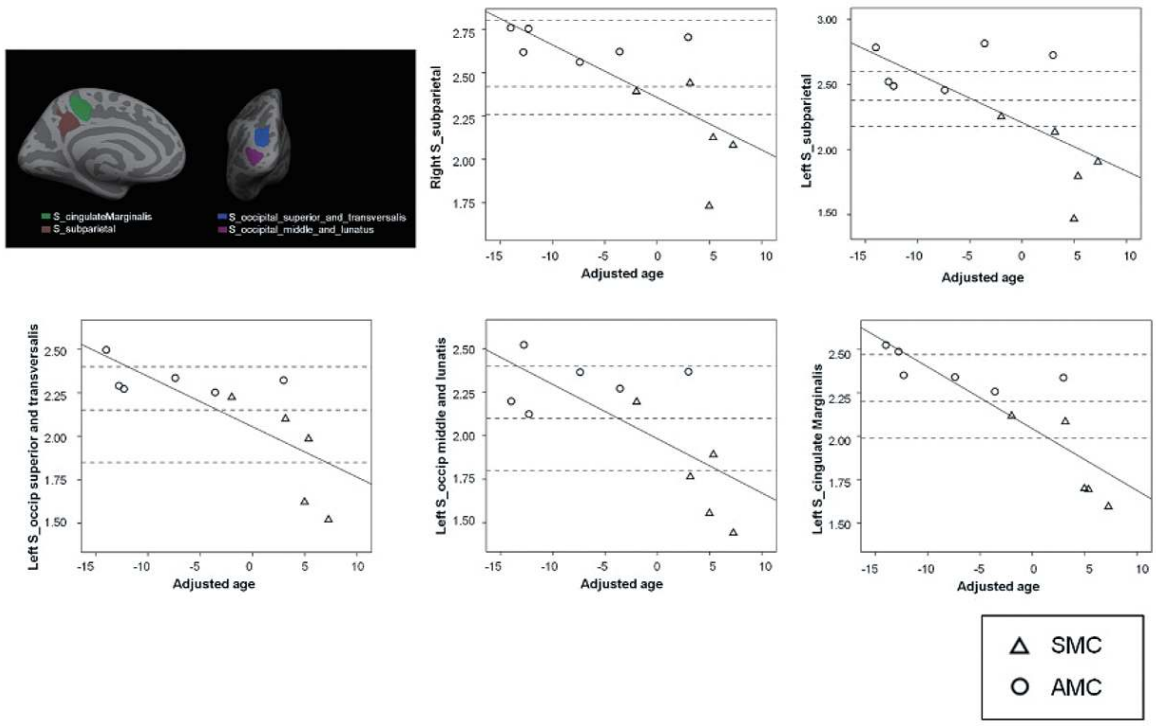

Fig. 6. Correlation between mean cortical thickness (CTh) values measured in several ROI obtained by the automated parcellation of the cortex available in FreeSurfer [16] and the adjusted age of each mutation carrier (asymptomatic carriers in circles and symptomatic carriers in triangles). Dashed lines represent the mean CTh measured in the same ROI for HC.

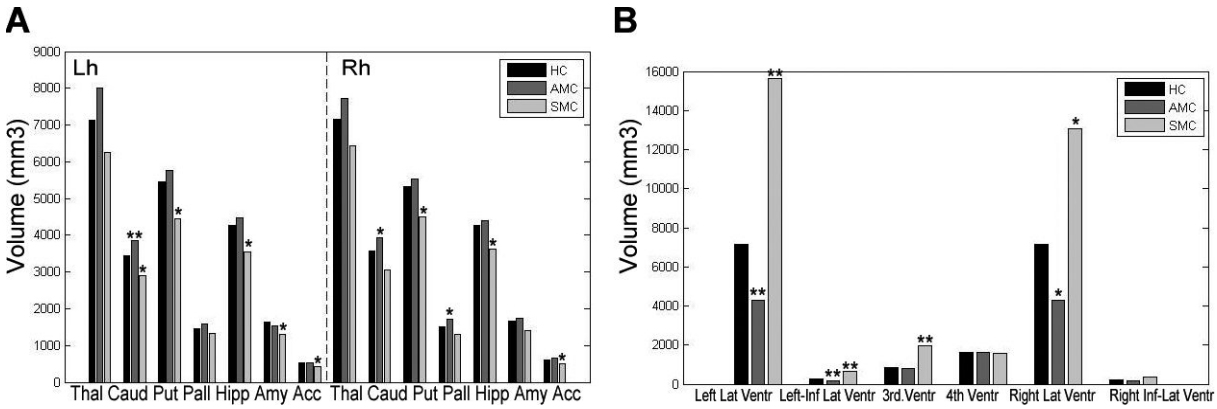

Fig. 7. (A) Volume of the atlas-based subcortical segmentations. Mean values within each group. (B) Volume of the atlas-based segmentation for ventricles and fluid-based segmentations. Mean values within each group. $^{*}p < 0.05$, $^{**}p < 0.01$ (group comparisons versus HC).

between individual CTh values and the adjusted age was found in MC ($r = 0.864$, $p = 0.006$, see Fig. 5). Only one AMC presented values far from the regression line. Interestingly, this subject was still asymptomatic at +3 years from predicted disease onset, a finding that shows the limitation of adjusted age as prediction of disease onset. The same type of results are obtained when analyzing this correlation in ROIs obtained with an automated parcellation of the cortex) [16] in areas of interest (Fig. 6).

Subcortical grey matter and ventricular volumes in symptomatic and asymptomatic mutation carriers

Atrophy in the SMC group, measured as a loss of grey matter, was significant in bilateral hippocampi,

Table 5
Average Mean Diffusivity measured in the two defined ROIs (SympROI and AsympROI), in the control ROI (VisualROI), and in subcortical structures. Caud: Caudate, Acc: Accumbens, Amy: Amygdala, Hipp: Hippocampus, Put: Putamen

MD (10^{-4} cm^2/s)	*SympROI* Mean (SD)	*AsympROI* Mean (SD)	*VisualROI* Mean (SD)	Caud Mean (SD)	Acc Mean (SD)	Amy Mean (SD)	Hipp Mean (SD)	Put Mean (SD)
HC	8.40 (0.55)	8.70 (0.56)	4.09 (0.53)	12.67 (1.76)	8.34 (0.46)	8.73 (0.28)	11.7 (0.63)	7.32 (0.36)
AMC	7.74 (0.28)	8.00 (0.56)	3.79 (0.57)	10.23 (1.46)	8.22 (0.56)	8.64 (0.28)	10.9 (0.36)	7.44 (0.27)
SMC	9.90 (0.43)	10.7 (8.77)	4.58 (0.67)	16.34 (0.80)	9.04 (0.75)	9.69 (1.12)	14.4 (1.53)	7.69 (0.31)
Group comparisons(*t-test*)								
SMC vs HC	$p < 0.001$	$p < 0.001$	$p = 0.11$	$p < 0.001$	$p = 0.02$	$p = 0.13$	$p = 0.016$	$p = 0.054$
HC vs AMC	$p = 0.028$	$p = 0.014$	$p = 0.28$	$p = 0.01$	$p = 0.64$	$p = 0.54$	$p = 0.018$	$p = 0.512$

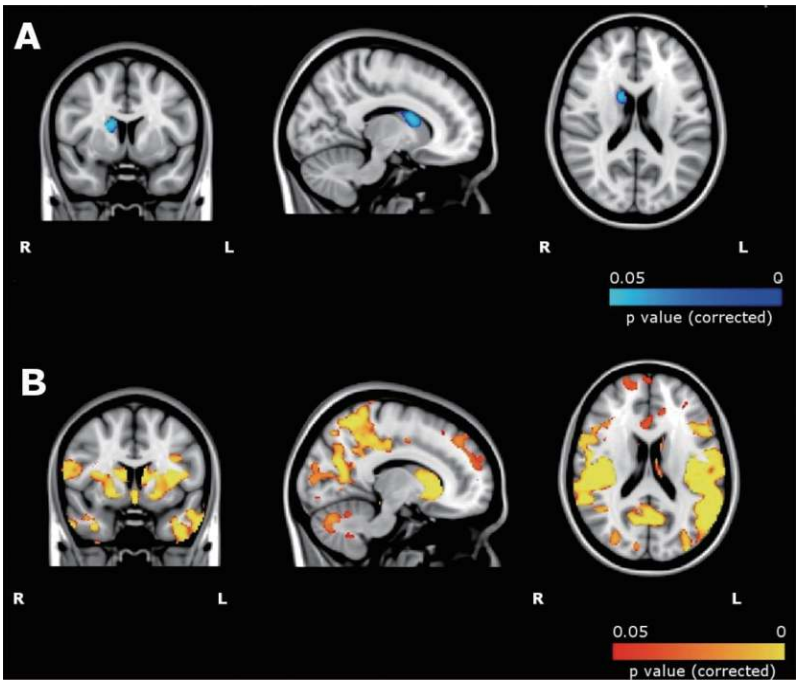

Fig. 8. VBM results. A) AMC versus HC ($p < 0.05$, corrected), (B) HC versus SMC ($p < 0.05$, corrected). Red-yellow color code means decreased volume, and blue color code means increased volume.

accumbens, putamen, and left caudate and amygdale with respect to HC. In contrast, AMC presented significant enlargement of the caudate bilaterally with respect to HC ($p < 0.01$ left caudate, $p < 0.05$ right caudate). Although without reaching statistical significance, many of the other atlas-based structures found to be atrophied in SMC were also enlarged in the AMC group (Fig. 7A).

Ventricular size showed the opposite trend. SMC showed a significant increase in ventricular size compared to HC whereas AMC showed significantly lower volumes. Moreover, these changes were found in the supratentorial compartment (lateral and third ventricles) with preservation of the 4th ventricle (Fig. 7B)

Voxel based morphometry analysis

VBM results are shown in Fig. 8. SMC showed significant widespread GM atrophy, mostly in PPC, parietotemporal association areas, lateral temporal ($p < 0.05$, corrected for multiple comparisons) and both caudates and bilateral putamen. AMC showed increased volume in right caudate. No areas were found enlarged in the SMC compared to HC or in the HC compared to the AMC.

Diffusivity indexes: Mean diffusivity in the cortex and caudate

The general linear model (GLM) analysis restricted to the cortex corrected for multiple comparisons across

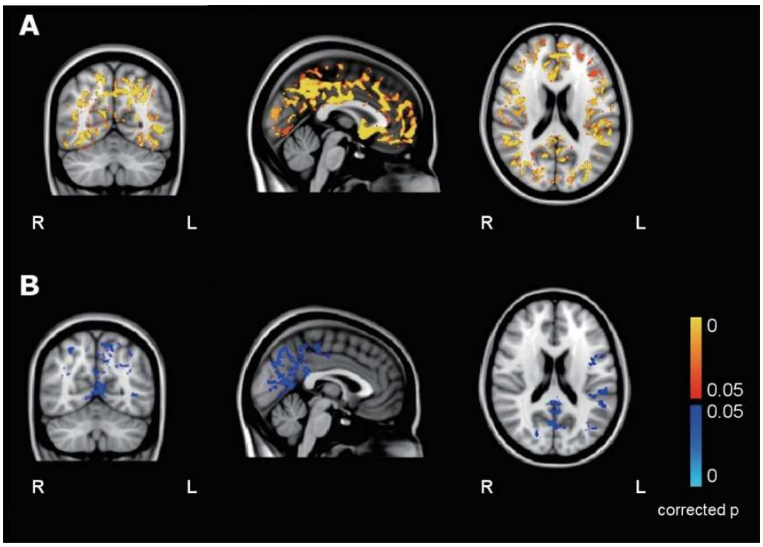

Fig. 9. A) Regions showing increased mean diffusivity (MD) in cortex in SMC versus HC (B). Regions showing reduced MD in cortex in AMC versus HC. Maps have been thresholded at $p < 0.05$, corrected.

space showed an increase in MD across the whole cerebral cortex in SMC compared to HC ($p < 0.05$ corrected). AMC presented changes in the opposite direction, with a decrease in MD mainly in PPC, cuneus and the IP (Fig. 9) compared to HC ($p < 0.05$, corrected).

To determine whether the areas that presented significant thickening co-localized with those areas with reduced diffusivity, MD was calculated in the *AsympROI*, *SympROI*, *VisualROI,* and several subcortical structures (Table 5). SMC showed a significant increase in MD in the *AsympROI* and *SympROI* (both $p < 0.001$) whereas AMC showed a significant decrease in MD ($p = 0.03$ and $p = 0.004$ respectively). The same trend of changes was also observed in subcortical structures (Table 5). Thus, in SMC, the caudates, accumbens, and hippocampi presented significant increases in MD whereas AMC showed significant decreases in MD in the caudates and hippocampi compared to HC. Neither SMC nor AMC showed differences in MD ($p = 0.11$ and $p = 0.28$ respectively) in the control area. In addition, when we fused MD in AMC with the areas that presented significant thickening in a sole figure (Fig. 10), the two areas showed a clear visual overlap.

DISCUSSION

We performed a study of structural and diffusivity indexes in cortical and subcortical grey matter in both symptomatic and asymptomatic *PSEN1* MC. SMC presented widespread cortical thinning in PPC and parietotemporal association areas in a pattern that resembles the "AD signature" of sporadic AD [7,8]. This pattern of GM cortical loss was already present at the non-demented stage, but to a much lesser extent similar to previous reports in sporadic AD [19]. Our results in SMC are consistent with, and expand on, previous findings in *PSEN1* and *AβPP* SMC. Hippocampal and global cerebral atrophy in SMC has been identified with volumetric MRI studies [5,6]. CTh has been shown to be decreased in several ROIs (entorhinal cortex, parahippocampal gyrus, PPC), but not in control regions in MC [9], demonstrating an accelerated decline in CTh in all target ROIs. In addition, in our study, the diffusivity analysis restricted to the GM in SMC replicated the expected findings [10], that is, an increase in MD across the whole cerebral cortex, target regions, and the subcortical structures affected.

In contrast, in AMC we found increased CTh in the PPC and parietotemporal association areas. This result was unexpected. For this reason and the fact that it was derived from the study of a small number of subjects (which constitutes the main limitation of the study) we performed several further analyses to support these findings. First, some areas survive multiple comparisons correction despite the small number of subjects in the sample. Second, the results at the individual level support the statistical analysis, as most AMC CTh individual mean values in the *AsympROI* fall outside the range of HC CTh. Third, CTh showed a significant correlation with the adjusted age of disease onset not only in the *AsympROI*, but also in several other ROIs

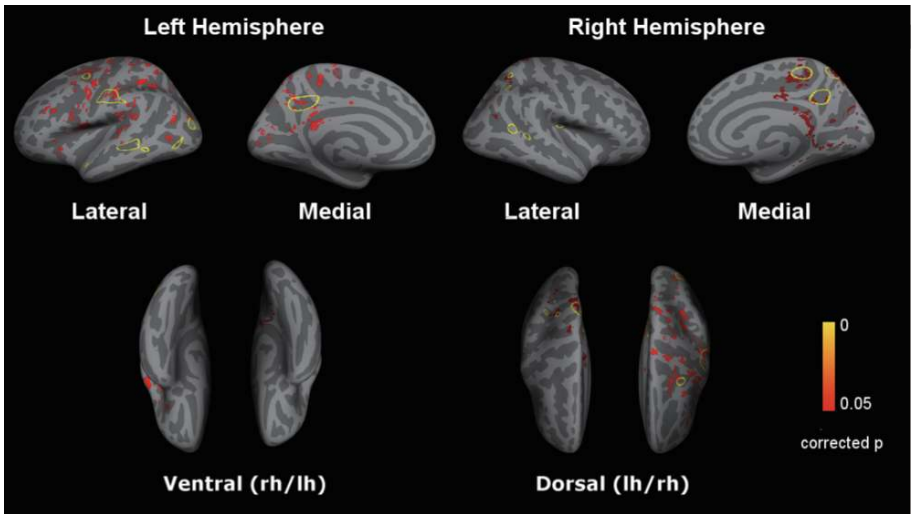

Fig. 10. Overlap of cortical thickness and mean diffusivity difference maps for AMC subjects. Green lines surround regions of cortical thickening ($p < 0.05$), and red-yellow regions are those where MD was found to be decreased in the AMC group. MD maps are mapped from volumetric to surface-based representation.

automatically extracted from FreeSurfer in the areas of interest, suggesting that the same areas found to be thickened suffer from thinning in MC as the disease progresses. Fourth, investigating the "specificity" of the areas involved, we found inverse changes in CTh in SMC and AMC in regions that present substantial visual overlap (*SympROI* and *AsympROI*), but not in the control region (*VisualROI*). Finally, the increase in CTh was accompanied by a significant fall in MD values, suggesting that not only gross structural changes but also microstructural abnormalities may be occurring.

To the best of our knowledge, this is the first report of increased CTh in *PSEN1* MC. Previous structural studies in AMC did not find differences, or suggested a loss of cortical GM in comparison with HC. There are two possible explanations for this discrepancy. First, if the shift from increased CTh towards atrophy is to happen in the asymptomatic phase of the disease, the results in each study would be critically dependent on the closeness to the predicted clinical onset of the AMC included in the sample. Our AMC are more distant from the predicted clinical onset (median adjusted age −9.9 years) than the subjects included in previous series (approximately −4 years) [6,9]. VBM studies have estimated that medial temporal atrophy and global atrophy begin 3 to 3.5 years before mean familial onset [5, 6] and longitudinal measures can identify differences in the rate of hippocampal GM loss in MC up to 5.5 years before diagnosis [5]. CTh decreased in posterior cingulate about 1.8 years and in the precuneus 4.1 years prior to diagnosis [9]. Second, technical differences may also account for the differences found, at least in part. Most previous studies have been performed with a volume-based registration approach instead of using a surface-based registration. CTh has been shown more accurate [14] and is a potentially more reliable marker than volume, as the cytoarchitectural structure of the grey matter is less variable [9]. Another advantage of CTh studies is that they may provide significant information even in small groups such as ours [20]. In fact, in the present study only CTh demonstrated cortical involvement when applying multiple comparisons correction and in the uncorrected results CTh demonstrated much more cortical involvement than VBM (data not shown).

Subcortical GM structures showed significant differences in the same direction, with significant increases in volume in both caudates in AMC, while SMC presented significant volume loss. The diffusivity analysis in the caudate in AMC showed significantly reduced MD. These results should be treated with caution because of possible CSF artifacts (especially MD results as the FSL VBM streamline already accounts for them in the volumetric analysis). Basal ganglia did not use to be considered among the typical areas affected in genetic AD but this idea changed after the demonstration of significant Aβ deposition in the striatum with much lower cortical deposition a decade before symptomatology onset in *PSEN1* AMC [21,22].

Several lines of evidence in the literature on morphometric studies in humans, pathological data, and studies in animal models support a possible increase in

CTh or subcortical GM volume in very early stages of AD. In a recent paper, *APOE* ε4 carriers showed thicker cortices than non-carriers, but a steeper age-related thinning in areas known to be affected in AD precisely in the life period (48–75 years old) when early morphological changes are beginning to emerge [23]. The authors interpreted the findings as a result of compensation of the underlying pathological processes. We believe that those results are very similar to ours and that the explanation presented there may also be applicable to our case. Moreover the same group has very recently replicated their results of cortical thickening in *APOE* ε4 carriers and reported that *APOE* ε4 related thickening modulates selective attention [24]. In pathological studies of cognitive normal subjects with changes of AD, cortical and hippocampal neurons show nuclear hypertrophy, interpreted as a probable reaction to Aβ, long before the onset of clinical symptoms [25,26]. The authors interpreted the results as either a compensatory response to AD pathology that prevents cognitive decline, or as a part of the pathological process. In animal models, a similar phenomenon was observed in transgenic mice, with neural hypertrophy and increased synaptic contacts reported in *AβPP*/PS1DeltaE9 animals [27,28]. Morphometric studies with serial MRI found an increase in cerebral and intracranial size in double transgenic mice [29]. The interpretation provided was that the results were a consequence of Aβ load and the associated inflammatory response (astrogliosis and microglial activation). In humans, inflammation has been reported very early in the course of the disease and there is evidence of complement activation on amyloid plaques in non-demented subjects who do not meet pathologic criteria for AD [30]. Immunotherapy trial results in AD also suggested that inflammation and Aβ load could account for GM thickness or volume, where the removal of Aβ (or other plaque-related proteins) and alterations in glial cell density have been suggested as explanations of the volume loss and ventricular enlargement found among antibody responders [31].

Both changes in cell volume or number produce an alteration in the cellular compartment with respect to the total volume within the cortex which may affect the diffusion of water measured with MD [32]. In our study, SMC presented the expected increase in MD in the cortex and caudate, probably as a reflection of neuronal loss [10]. In contrast, AMC showed a significant decrease in MD, which may have reflected the increase in both cell volume and number due to an inflammatory response. Thus, either reactive neuronal hypertrophy or inflammatory response to Aβ, or probably both, could account for the increased CTh or volume and decreased MD found in AMC in our study.

Notwithstanding the absence of previous reports of cortical thickening in genetic AD, in Huntington disease (HD) cortical volume or thickness has been found significantly increased in far-from-onset preclinical HD [33] and YAC128 mice [34]. Paulsen and colleagues [33] underlined the possibility of an abnormal cortical development to explain the increased cortical volume. Lerch et al. [34] also suggested the possibility of a compensatory response to striatal degeneration or some type of inflammatory response preceding cell death in accordance with neuropathological data on preclinical HD [35], which coincides with the interpretation we give to our findings. Whatever the interpretation both the findings in HD and our present results expand the ability of structural neuroimaging from detecting atrophy to actually detecting gray matter increases at earlier stages of neurodegenerative disorders.

On the other hand, while SMC presented abnormal Aβ mean values, AMC Aβ values were normal, suggesting that in these subjects Aβ fibrillar deposition was not severe or extensive enough to produce a reduction in CSF Aβ levels [36]. Nevertheless, morphometric and microstructural changes in AMC could be mediated by the toxic effect of Aβ oligomers or diffuse plaques previous to Aβ fibrillar deposition. However, the small number of subjects studied and the lack of amyloid imaging data to evaluate focal fibrillar Aβ deposition requires us to be extremely cautious with this interpretation.

Recently, Jack and colleagues summarized the currently available evidence on sporadic AD and proposed a model that related disease stage to AD biomarkers [37]. In their model, a preclinical phase of the disease corresponds to the deposition of fibrillar Aβ marked by reductions in CSF Aβ and increased amyloid PET tracer retention. Neurodegeneration appeared later marked with functional abnormalities, increased CSF tau and atrophy in MRI. The finding of increased CTh and caudate volume with normal values of Aβ does not fit either of the stages described in Jack's model. Although we should bear in mind that the model was proposed for sporadic AD and the sequence of events in these two populations may differ, our findings could in fact fit the model if we place our AMC subjects at the very beginning of the β-amyloidosis phase or in a previous one, driven by soluble Aβ. As the designers of this model acknowledged, features such as the role of toxic Aβ oligomeric species or diffuse plaques and the timing of their appearance were not included, as there are currently no reliable biomarkers for them.

Our study has several limitations. As mentioned above the first and most important is the small number of subjects studied, although in rare genetic populations this is practically inevitable. Therefore we should emphasize that it will be essential to replicate our findings in other cohorts to confirm our results. Another limitation in the interpretation of these results is the use of adjusted age as theoretical construct to substitute currently unknown real age of onset. We acknowledge that the absence of Aβ imaging, which is not currently available, is another limitation in the interpretation of the results. As discussed above, the study of CSF Aβ levels was performed to overcome, at least in part, this problem [37]. In spite of these limitations, we believe that our findings are robust and can be interpreted in accordance with previous data. There is a great research effort devoted to finding imaging biomarkers of early pathological changes in AD and the present work may have important implications in this area. However, the degree to which they can be extrapolated to sporadic AD remains unknown.

In conclusion, CTh appears to be increased in the precuneus and parietotemporal association areas in *PSEN1* MC during early preclinical stages of the disease. Subcortical GM structures, especially the caudate nucleus, are also enlarged. With disease progression, these areas suffer GM loss and become thinner or atrophied. The increase in mean CTh and caudate volumes in AMC is associated with a decrease in MD, whereas atrophy in SMC is associated with increased MD. The inverse changes in diffusion indices in SMC and AMC suggest different microstructure abnormalities underlying the contrasting morphometric findings. Reactive neuronal hypertrophy or inflammatory response to Aβ, or both, may account for the increased CTh and decreased MD found in AMC whereas decreased CTh and increased MD in SMC may reflect predominant neuronal loss.

ACKNOWLEDGMENTS

This study has been funded by research grants from the *Instituto Carlos III* (FIS080036) and from the Spanish *Ministerio de Ciencia e Innovación* (SAF2009-07489), Spain. Juan Fortea is the receptor of a Josep Font grant from Hospital Clinic. We thank Michael Maudsley for help with the English and thank all the volunteers for their participation in this study.

Sources of support: Dr Juan Fortea reports having received a Josep Font grant from Hospital Clinic. Dr Raquel Sanchez-Valle has received a grant (FIS080036) from the Spanish *Ministerio de Ciencia e Innovación.*

Authors' disclosures available online (http://www.j-alz.com/disclosures/view.php?id=558).

REFERENCES

[1] Alzheimer Disease & Frontotemporal Dementia Mutation Database, http://www.molgen.ua.ac.be/admutations/, Accessed on February 2, 2010.

[2] Mondadori CR, Buchmann A, Mustovic H, Schmidt CF, Boesiger P, Nitsch RM, Hock C, Streffer J, Henke K (2006). Enhanced brain activity may precede the diagnosis of Alzheimer's disease by 30 years. *Brain* **129**, 2908-2922.

[3] Godbolt AK, Waldman AD, MacManus DG, Schott JM, Frost C, Cipolotti L, Fox NC, Rossor MN (2006) MRS shows abnormalities before symptoms in familial Alzheimer disease. *Neurology* **66**, 718-722.

[4] Schott JM, Fox NC, Frost C, Scahill RI, Janssen JC, Chan D, Jenkins R, Rossor MN (2003) Assessing the onset of structural change in familial Alzheimer's disease. *Ann Neurol* **53**, 181-188.

[5] Ridha BH, Barnes J, Bartlett JW, Godbolt A, Pepple T, Rossor MN, Fox NC (2006) Tracking atrophy progression in familial Alzheimer's disease: a serial MRI study. *Lancet Neurol* **5**, 828-834.

[6] Mosconi L, Sorbi S, de Leon MJ, Li Y, Nacmias B, Myoung PS, Tsui W, Ginestroni A, Bessi V, Fayyazz M, Caffarra P, Pupi A (2006) Hypometabolism exceeds atrophy in presymptomatic early-onset familial Alzheimer's disease. *J Nucl Med* **47**, 1778-1786.

[7] Desikan RS, Cabral HJ, Hess CP, Dillon WP, Glastonbury CM, Weiner MW, Schmansky NJ, Greve DN, Salat DH, Buckner RL, Fischl B; Alzheimer's Disease Neuroimaging Initiative (2009) Alzheimer's Disease Neuroimaging Initiative. Automated MRI measures identify individuals with mild cognitive impairment and Alzheimer's disease. *Brain* **132**, 2048-2057.

[8] Dickerson BC, Bakkour A, Salat DH, Feczko E, Pacheco J, Greve DN, Grodstein F, Wright CI, Blacker D, Rosas HD, Sperling RA, Atri A, Growdon JH, Hyman BT, Morris JC, Fischl B, Buckner RL (2009) The cortical signature of Alzheimer's disease: regionally specific cortical thinning relates to symptom severity in very mild to mild AD dementia and is detectable in asymptomatic amyloid-positive individuals. *Cereb Cortex* **19**, 497-510.

[9] Knight WD, Kim LG, Douiri A, Frost C, Rossor MN, Fox NC (2010) Acceleration of cortical thinning in familial Alzheimer's disease. *Neurobiol Aging*, in press.

[10] Müller MJ, Greverus D, Weibrich C, Dellani PR, Scheurich A, Stoeter P, Fellgiebel A (2007) Diagnostic utility of hippocampal size and mean diffusivity in amnestic MCI. *Neurobiol Aging* **28**, 398-403.

[11] Carlesimo GA, Cherubini A, Caltagirone C, Spalletta G (2010) Hippocampal mean diffusivity and memory in healthy elderly individuals: a cross-sectional study. *Neurology* **74**, 194-200.

[12] Sánchez-Valle R, Lladó A, Ezquerra M, Rey MJ, Rami L, Molinuevo JL (2007) A novel mutation in the PSEN1 gene (L286P) associated with familial early-onset dementia of Alzheimer type and lobar haematomas. *Eur J Neurol* **14**, 1409-1412.

[13] Lladó A, Fortea J, Ojea T, Bosch B, Sanz P, Valls-Solé J, Clarimon J, Molinuevo JL, Sánchez-Valle R (Epub ahead of print) A

novel PSEN1 mutation (K239N) associated with Alzheimer's disease with wide range age of onset and slow progression. *Eur J Neurol* **17**, 994-996

[14] Fischl B, Dale AM (2000) Measuring the thickness of the human cerebral cortex from magnetic resonance images. *Proc Natl Acad Sci U S A* **97**, 11050-11055.

[15] Desikan RS, Ségone F, Fischl B, Quinn BT, Dickerson BC, Blacker D, Buckner RL, Dale AM, Maguire RP, Hyman BT, Albert MS, Killiany RJ (2006). An automated labelling system for subdividing the human cerebral cortex on MRI scans into gyral based regions of interest. *Neuroimage* **31**, 968-980.

[16] Fischl B, van der Kouwe A, Destrieux C, Halgren E, Ségonne F, Salat DH, Busa E, Seidman LJ, Goldstein J, Kennedy D, Caviness V, Makris N, Rosen B, Dale AM (2004). Automatically parcellating the human cerebral cortex. *Cereb Cortex* **14**, 11-22.

[17] Buckner RL, Head D, Parker J, Fotenos AF, Marcus D, Morris JC, Snyder AZ (2004). A unified approach for morphometric and functional data analysis in young, old, and demented adults using automated atlas-based head size normalization: reliability and validation against manual measurement of total intracranial volume. *Neuroimage* **23**, 724-738.

[18] Smith SM, Jenkinson M, Woolrich MW, Beckmann CF, Behrens TE, Johansen-Berg H, Bannister PR, De Luca M, Drobnjak I, Flitney DE, Niazy RK, Saunders J, Vickers J, Zhang Y, De Stefano N, Brady JM, Matthews PM (2004) Advances in functional and structural MR image analysis and implementation as FSL. *Neuroimage* **23**, S208-S219.

[19] Whitwell JL, Shiung MM, Przybelski SA, Weigand SD, Knopman DS, Boeve BF, Petersen RC, Jack CR Jr (2008) MRI patterns of atrophy associated with progression to AD in amnestic mild cognitive impairment. *Neurology* **70**, 512-520.

[20] Eskildsen SF, Østergaard LR, Rodell AB, Østergaard L, Nielsen JE, Isaacs AM, Johannsen P (2009) Cortical volumes and atrophy rates in FTD-3 CHMP2B mutation carriers and related non-carriers. *Neuroimage* **45**, 713-721.

[21] Klunk WE, Price JC, Mathis CA, Tsopelas ND, Lopresti BJ, Ziolko SK, Bi W, Hoge JA, Cohen AD, Ikonomovic MD, Saxton JA, Snitz BE, Pollen DA, Moonis M, Lippa CF, Swearer JM, Johnson KA, Rentz DM, Fischman AJ, Aizenstein HJ, DeKosky ST (2007) Amyloid deposition begins in the striatum of presenilin-1 mutation carriers from two unrelated pedigrees. *J Neurosci* **27**, 6174-6184.

[22] Villemagne VL, Ataka S, Mizuno T, Brooks WS, Wada Y, Kondo M, Jones G, Watanabe Y, Mulligan R, Nakagawa M, Miki T, Shimada H, O'Keefe GJ, Masters CL, Mori H, Rowe CC (2009) High striatal amyloid beta-peptide deposition across different autosomal Alzheimer disease mutation types. *Arch Neurol* **66**, 1537-1544.

[23] Espeseth T, Westlye LT, Fjell AM, Walhovd KB, Rootwelt H, Reinvang I (2008) Accelerated age-related cortical thinning in healthy carriers of apolipoprotein E epsilon 4. *Neurobiol Aging* **29**, 329-340.

[24] Espeseth T, Westlye LT, Walhovd KB, Fjell AM, Endestad T, Rootwelt H, Reinvang I (2010) Apolipoprotein E epsilon4-related thickening of the cerebral cortex modulates selective attention. *Neurobiol Aging*, in press.

[25] Riudavets MA, Iacono D, Resnick SM, O'Brien R, Zonderman AB, Martin LJ, Rudow G, Pletnikova O, Troncoso JC (2007) Resistance to Alzheimer's pathology is associated with nuclear hypertrophy in neurons. *Neurobiol Aging* **28**, 1484-1492.

[26] Iacono D, Markesbery WR, Gross M, Pletnikova O, Rudow G, Zandi P, Troncoso JC (2009) The Nun study: clinically silent AD, neuronal hypertrophy, and linguistic skills in early life. *Neurology* **73**, 665-673.

[27] West MJ, Bach G, Søderman A, Jensen JL (2009) Synaptic contact number and size in stratum radiatum CA1 of APP/PS1DeltaE9 transgenic mice. *Neurobiol Aging* **30**, 1756-1776.

[28] Oh ES, Savonenko AV, King JF, Fangmark Tucker SM, Rudow GL, Xu G, Borchelt DR, Troncoso JC (2009) Amyloid precursor protein increases cortical neuron size in transgenic mice. *Neurobiol Aging* **30**, 1238-1244.

[29] Maheswaran S, Barjat H, Rueckert D, Bate ST, Howlett DR, Tilling L, Smart SC, Pohlmann A, Richardson JC, Hartkens T, Hill DL, Upton N, Hajnal JV, James MF (2009) Longitudinal regional brain volume changes quantified in normal aging and Alzheimer's APP x PS1 mice using MRI. *Brain Res* **1270**, 19-32.

[30] Zanjani H, Finch CE, Kemper C, Atkinson J, McKeel D, Morris JC, Price JL (2005) Complement activation in very early Alzheimer disease. *Alzheimer Dis Assoc Disord* **19**, 55-66.

[31] Fox NC, Black RS, Gilman S, Rossor MN, Griffith SG, Jenkins L, Koller M; AN1792(QS-21)-201 Study (2005) Effects of Abeta immunization (AN1792) on MRI measures of cerebral volume in Alzheimer disease. *Neurology* **64**, 1563-1572.

[32] Sotak CH. Nuclear magnetic resonance (NMR) measurement of the apparent diffusion coefficient (ADC) of tissue water and its relationship to cell volume changes in pathological states. *Neurochem Int* **45**, 569-582.

[33] Paulsen JS, Magnotta VA, Mikos AE, Paulson HL, Penziner E, Andreasen NC, Nopoulos PC (2006) Brain structure in preclinical Huntington's disease. *Biol Psychiatry* **59**, 57-63.

[34] Lerch JP, Carroll JB, Dorr A, Spring S, Evans AC, Hayden MR, Sled JG, Henkelman RM (2008) Cortical thickness measured from MRI in the YAC128 mouse model of Huntington's disease. *Neuroimage* **41**, 243-251.

[35] Gómez-Tortosa E, MacDonald ME, Friend JC, Taylor SA, Weiler LJ, Cupples LA, Srinidhi J, Gusella JF, Bird ED, Vonsattel JP, Myers RH (2001) Quantitative neuropathological changes in presymptomatic Huntington's disease. *Ann Neurol* **49**, 29-34.

[36] Fagan AM, Mintun MA, Mach RH, Lee SY, Dence CS, Shah AR, LaRossa GN, Spinner ML, Klunk WE, Mathis CA, DeKosky ST, Morris JC, Holtzman DM (2006) Inverse relation between in vivo amyloid imaging load and cerebrospinal fluid Abeta42 in humans. *Ann Neurol* **59**, 512-59.

[37] Jack CR Jr, Knopman DS, Jagust WJ, Shaw LM, Aisen PS, Weiner MW, Petersen RC, Trojanowski JQ (2010) Hypothetical model of dynamic biomarkers of the Alzheimer's pathological cascade. *Lancet Neurol* **9**, 119-128.